Chemosphere 325 (2023) 138414

Contents lists available at ScienceDirect

Chemosphere

journal homepage: www.elsevier.com/locate/chemosphere

Reductive transformation of birnessite by low-molecular-weight organic acids

Thomas Ritschel, Kai Uwe Totsche *

Department of Hydrogeology, Institute for Geosciences, Friedrich Schiller University Jena, Burgweg 11, 07749, Jena, Germany

HIGHLIGHTS

- Birnessite reductively transforms into feitknechtite and manganite.
- Low-molecular-weight organic acids readily oxidize in presence of manganese oxides.
- Organic acids oxidize from lactate to pyruvate, acetate, oxalate, and inorganic C.
- Multivariate statistics of XRD and FTIR spectra reveals mineral phase transitions.
- Abiotic alteration thermodynamically stabilizes pedogenic manganese phases.

GRAPHICAL ABSTRACT

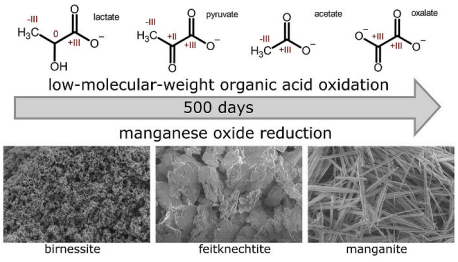

ARTICLE INFO

Handling Editor: T Cutright

Keywords:
Feitknechtite
Manganite
X-ray diffraction (XRD)
Fourier-transform infrared spectroscopy (FTIR)
Linear combination fit (LCF)

ABSTRACT

Soil biogeochemistry is intrinsically coupled to the redox cycling of iron and manganese. Oxidized manganese forms various (hydr)oxides that may reductively transform and dissolve, thereby serving as electron acceptors for microbial metabolisms. Furthermore, manganese oxides might reduce purely abiotically by oxidation of dissolved Mn^{2+} in a specific route of transformation from birnessite ($Mn^{IV}O_2$) into metastable feitknechtite (β-$Mn^{III}OOH$) and stable manganite (γ-$Mn^{III}OOH$). In natural soil solutions, however, dissolved Mn^{2+} is not abundant and organic substances such as low-molecular-weight organic acids (LMWOA) may be oxidized and serve as an electron donor for manganese oxide reduction instead. We investigated whether LMWOA would impact the transformation of birnessite at a temperature of 290 $\pm$ 2 K under ambient pressure for up to 1200 d. We found that birnessite was reductively transformed into feitknechtite, which subsequently alters into the more stable manganite without releasing Mn^{2+} into the solution. Instead, LMWOA served as electron donors and were oxidized from lactate into pyruvate, acetate, oxalate, and finally, inorganic carbon. We conclude that the reductive transformation of short-range ordered minerals like birnessite by the abiotic oxidation of LMWOA is a critical process controlling the abundance of LMWOA in natural systems besides their microbial consumption. Our results further suggest that the reduction of Mn^{IV} oxides not necessarily results in their dissolution at neutral and alkaline pH but also forms more stable Mn^{III} oxyhydroxides with less oxidative degradation potential for organic contaminants.

* Corresponding author. Department of Hydrogeology, Institute for Geosciences, Friedrich Schiller University Jena, Burgweg 11, 07749, Jena, Germany.
E-mail address: kai.totsche@uni-jena.de (K.U. Totsche).

https://doi.org/10.1016/j.chemosphere.2023.138414
Received 23 September 2022; Received in revised form 23 February 2023; Accepted 13 March 2023
Available online 14 March 2023

1. Introduction

Manganese oxides are ubiquitous minerals with high redox-reactivity in the environment and are formed, altered, and dissolved by abiotic and biotic reactions (Borch et al., 2010; Post, 1999; Yang et al., 2021). They play an essential role in many biogeochemical processes, such as the sorption of metals or nutrients and the oxidation of inorganic and organic contaminants (Borch et al., 2010; Hem, 1978; Jones et al., 2018; Remucal and Ginder-Vogel, 2014; Tebo et al., 2004). Birnessite, one of the most common Mn^{IV} oxides in soils and aquatic systems (Bargar et al., 2009; Jones and Milne, 1956; Taylor, 1968; Wang et al., 2012), is frequently the first Mn phase that forms and acts as a precursor for several other Mn oxides (Tebo et al., 2004). Birnessite is known to, e.g., oxidize As^{III} to As^{V}, thus reducing its mobility as well as toxicity (Manning et al., 2002), and convert $[Fe^{II}(CN)_6]^{4-}$ to $[Fe^{III}(CN)_6]^{3-}$, preventing it from releasing toxic CN^- into solution (Rennert et al., 2005).

In soils, aquatic sediments, and shallow aquifers, Mn^{IV} oxides – similar to iron oxides – may serve as electron acceptors once other readily available electron acceptors, e.g., O_2, and NO_3^-, are consumed by the oxidative microbial decomposition of organic matter (Nealson and Saffarini, 1994). Consequently, manganese oxides dissolve and release Mn^{2+} and metal ions bound to manganese oxides into the environment (Burdige et al., 1992; Lovley, 1991; Mansfeldt, 2004). Recent studies proposed that besides Mn^{2+}, soluble Mn^{3+} is released into porewater under suboxic conditions as well (Fritzsche et al., 2016; Madison et al., 2013). Dissolved Mn^{2+} is capable of reducing birnessite by a comproportionation into metastable Mn^{III} oxides such as feitknechtite that subsequently transforms into manganite at pH 7–8 under ambient temperature and pressure conditions (Elzinga, 2011; Lefkowitz et al., 2013; Luo et al., 1998; Tu et al., 1994). Such a transformation stabilizes manganese in soils because the newly formed feitknechtite and manganite are thermodynamically more stable than birnessite and, thus, less susceptible to reductive dissolution (Bricker, 1965). However, their lower reactivity compared to birnessite also limits their capacity to oxidize soil pollutants. Furthermore, the formation of thermodynamically more stable mineral phases is crucial in pedogenesis to establish the mineral composition in mature soil. Yet, in natural soil solutions, Mn^{2+} concentrations that facilitate such manganese transformations (Elzinga, 2011) are very low. Instead, a variety of organic substances, e.g., low molecular-weight organic acids (LMWOA) such as oxalate, lactate, pyruvate, and acetate, are present (Jones, 1998) that are known to reductively dissolve manganese oxides and release Mn^{2+} (Stone, 1987; Wang and Stone, 2006b; Xyla et al., 1992). The associated reduction rates, however, sharply diminish when the pH is not acidic, and hardly any reductive dissolution is observed at neutral or alkaline pH, where manganese oxidation is favored instead (Hem, 1981). However, manganese oxide reduction can be induced even at alkaline pH by anaerobic LMWOA consumption (Novotnik et al., 2019). Furthermore, Flynn and Catalano (2019) found clear evidence that LMWOA oxidization in the presence of manganese oxides at circumneutral pH changes the average manganese oxidation state in birnessite and, therefore, also induces transformations in the crystal structure. However, no transition to other manganese phases was observed after 28 days, and it remains unclear if LMWOA might participate in the transformation of manganese oxides like dissolved Mn^{2+}. Furthermore, the abiotic transformation of birnessite has been observed in the presence of fulvic acids (Wang et al., 2018). Hence, the purely abiotic transformation of manganese oxides is also suggested in the presence of LMWOA. In this context, the low concentration of LMWOA in soil solutions and the presence of altered manganese phases may partly be attributed to the reduction of manganese oxides by LMWOA that serve as the electron donor.

In a previous study by Händel et al. (2013a), LMWOA were used to synthesize birnessite by reducing permanganate with lactate, an ubiquitous low-molecular-weight organic acid. Here, we follow up on that experiment by examining the influence of lactate and its oxidation products on the reductive transformation of birnessite synthesized this way over extended periods. Furthermore, as the exact route of Mn^{IV} oxide transformation due to LMWOA has not been studied yet, we explored the role of LMWOA in the reductive transformation of Mn oxides in response to the availability of LMWOA. Specifically, we followed the transformation up to 1200 d under abiotic conditions by combining $KMnO_4$ with Na-lactate in various ratios, from concentrations that fully consume lactate to concentrations where lactate is present in excess.

2. Materials and methods

2.1. Manganese oxide synthesis

A solution of permanganate was treated with three concentrations of lactate by preparing 25 mL of a 63.3 mM $KMnO_4$ (Carl Roth, Karlsruhe, Germany, p.a.) solution with 31.7 mM (Mix 1:2), 63.3 mM (Mix 1:1), or 126.7 mM (Mix 2:1) Na-lactate (prepared from Na-Lactate 50%; $\rho = 1.26\ g\ cm^{-3}$, VWR-Prolabo, Darmstadt, Germany) similar to the method of Händel et al. (2013a) to facilitate the formation of an initial birnessite phase. Accordingly, the stoichiometric ratios between lactate and MnO_4^- were 1:2, 1:1, and 2:1, respectively. The stoichiometric ratios were chosen such that permanganate reduction to birnessite entirely consumes lactate and its potential reaction product pyruvate at the lowest lactate concentration. At higher lactate input, lactate is provided in excess such that lactate is not entirely consumed, and pyruvate not necessarily oxidizes upon birnessite formation. The solutions were stored at a temperature of 290 ± 2 K under ambient pressure in the dark and shaken once a week for a total period of 1, 2, 3, 5, 7, 10, 25, 50, 100, 199, 500, and 1200 d. Additional mixtures containing only Na-lactate or $KMnO_4$ were set up as controls for all time steps. For all time steps, three replicates were prepared. At every sampling time, the suspension was centrifuged to separate the solids from the solution. The supernatant was filtered (0.45 μm) and used for characterizing the solution. The solid was washed five times with purified water to remove residual ions and freeze-dried for further analyses. Ultrapure water (R = 18.2 MΩ, DOC $<1\ \mu g\ L^{-1}$, Elix + Milli Q, Millipore, Billerica, MA, USA) was used for all sample preparations, dilution series, and purification steps.

2.2. Solution chemistry

The pH of the solutions was measured directly after filtration (Sentix 41 + pH 197i, WTW, Weilheim, Germany). Dissolved inorganic carbon (DIC) was determined by means of CO_2 released after sample acidification with H_3PO_4 (Multi N/C 2100, Analytik Jena, Jena, Germany). After acidification with HCl and purging with C-free air, the dissolved organic carbon (DOC) was determined by combustion (Multi N/C 2100, Analytik Jena, Jena, Germany). Organic anions (lactate, pyruvate, acetate, and oxalate) were determined with ion chromatography (EG50, Dionex, Brunsbüttel, Germany) equipped with ion-selective columns (AG11-HC, Column Manufacturer, Dornden, Swiss) using KOH as the eluent and a conductivity detector (CD20, Dionex, Brunsbüttel, Germany). Additionally, after 1, 10, 100, 199, and 500 d, the Na, K, Mg, Ca, Mn, and Fe concentrations were analyzed by inductively coupled plasma optical emission spectroscopy (Varian 725-ICP-OES, Varian, USA).

2.3. Characterization of synthesis products

X-ray diffractograms were obtained with a Bruker D8 Advance DaVinci diffractometer (Bruker AXS, Karlsruhe, Germany) using Cu-Kα radiation (λ = 0.15418 nm) at 40 kV and 40 mA, step-scanning from 5 to 90 °2θ with a step size of 0.04 °2θ and a counting time of 1 s per step. In addition, Fourier-transform infrared (FTIR) spectra were recorded with a Nicolet iS10 spectrometer (Thermo Fisher Scientific, Dreieich, Germany) using mortared samples mixed with KBr at a ratio of 1:100 and

pressed to pellets. The pellets were measured in transmission mode in the mid-infrared range between 4000 and 400 cm^{-1} for 16 scans at a resolution of 4 cm^{-1}.

The alteration of spectra suggests a succession of manganese phases where spectra in periods of mineral transformation are superpositions of pure mineral phase spectra that can be quantified efficiently with multivariate statistical methods. Hence, we applied a Linear Combination Fit (LCF) using three components since pure mineral spectra were available after 1 d, 100 d, and 500 d for birnessite, feitknechtite, and manganite, respectively. The LCF was calculated using nonnegativity-constrained linear regression (Fritzsche et al., 2019; Ritschel and Totsche, 2017) to ascertain that components cannot compensate each other with negative contents.

From all samples, scanning electron microscopy images were obtained with an ULTRA plus field emission scanning electron microscope (Zeiss, Jena, Germany). All samples were placed on Si wafers.

3. Results and discussion

3.1. Transformation of mineral phases

In all treatments (Mix 1:2, Mix 1:1, Mix 2:1), a precipitate readily formed after 1 d. According to the X-ray diffraction patterns (Fig. 1) and infrared spectra (Fig. 2), an initial birnessite showing the same features as found after the reduction of permanganate with lactate by Händel et al. (2013a) has formed. Broad asymmetrical XRD reflexes seen in Fig. S1 at 12.0 °2θ (7.2 Å), 24.7 °2θ (3.6 Å), 37.2 °2θ (2.4 Å), and 66.1 °2θ (1.4 Å) also match with other routes of synthesis (McKenzie, 1971). Therefore, we assume that a similar birnessite structure has formed, showing turbostratic stacking of the birnessite layers with an alternation of one-layer hexagonal and one-layer monoclinic MnO_6 octahedra (Händel et al., 2013a). Similarly, the IR absorption bands at 519 and 452 cm^{-1} caused by the lattice vibrations of the MnO_6 octahedra, as well as the bands at 3419 and 1627 cm^{-1} (Fig. S1) attributed to either adsorbed H_2O or H_2O in the interlayer regions of birnessite (Julien et al., 2004; Potter and Rossman, 1979) are similar to previous findings (Händel et al., 2013a). The birnessite initially formed in all treatments consists of tiny colloidal crystals combined into aggregates with a micro-porous structure (Fig. 3a, S2) similar to those found by Händel et al. (2013a). In Mix 1:2, the spectra and diffractograms found after 1 d remain unchanged over the entire period of the experiment (1–1200 d, Figs. S3–4).

In Mix 1:1 and Mix 2:1, diffraction reflexes that indicate the presence of a well crystalline manganese phase emerge at 19.0 °2θ (4.7 Å), 33.3 °2θ (2.7 Å), and 37.8 °2θ (2.4 Å) 46.1 °2θ (2.0 Å) after 2–3 d, and are fully formed after 10–25 d (Fig. 1). These reflexes match with those found for the Mn^{III} oxide feitknechtite (Anthony et al., 1997) and indicate the reductive transformation of birnessite induced by the oxidation of LMWOA that are left after the initial reduction of permanganate (for a detailed discussion of the role of different LMWOA see section 3.3). This interpretation is supported by FTIR absorption bands formed at 1071 and 946 cm^{-1} (Fig. 2), which are characteristic of bending vibrations of the OH groups found in feitknechtite, while the lattice vibrations of the MnO_6 octahedra have shifted to 600 and 448 cm^{-1} (Elzinga, 2011). In addition, several more XRD reflexes evolve at 39.6 °2θ (2.3 Å), 40.4 °2θ (2.2 Å), 44.0 °2θ (2.1 Å), 49.3 °2θ (1.9 Å), 53.7 °2θ (1.7 Å), 56.0 °2θ and 58.6 °2θ (1.6 Å) that do not appear in XRD references for feitknechtite. Yet, Mandernack et al. (1995) found a very similar XRD pattern after microbial oxidation of Mn^{2+} that features the same reflexes as the feitknechtite formed in our experiments. As the morphology of the manganese phase developed into stacked sheets of very thin layers (Fig. 3b) that are typical for feitknechtite, we assume that a very crystalline feitknechtite phase has evolved with other reflexes that have not been described before.

In Mix 1:1 and Mix 2:1, the XRD spectra remain unchanged until 100 days. After 100–199 d, other reflexes emerge at 26.2 °2θ (3.4 Å), 33.9 °2θ (2.6 Å), 35.6 °2θ (2.5 Å), 37.2 °2θ (2.4 Å), 51.2 °2θ (1.8 Å) and 54.9 °2θ (1.7 Å) (Fig. 1) that are characteristic reflexes for manganite (Anthony et al., 1997; Buerger, 1936). At 1190 and 1150 cm^{-1}, the in-plane bending vibrations, and at 1085 cm^{-1} (Fig. 2), the out-of-plane bending vibrations of OH groups in the manganite evolve (Kohler et al., 1997), while the lattice vibrations of the MnO_6 octahedra have now shifted to

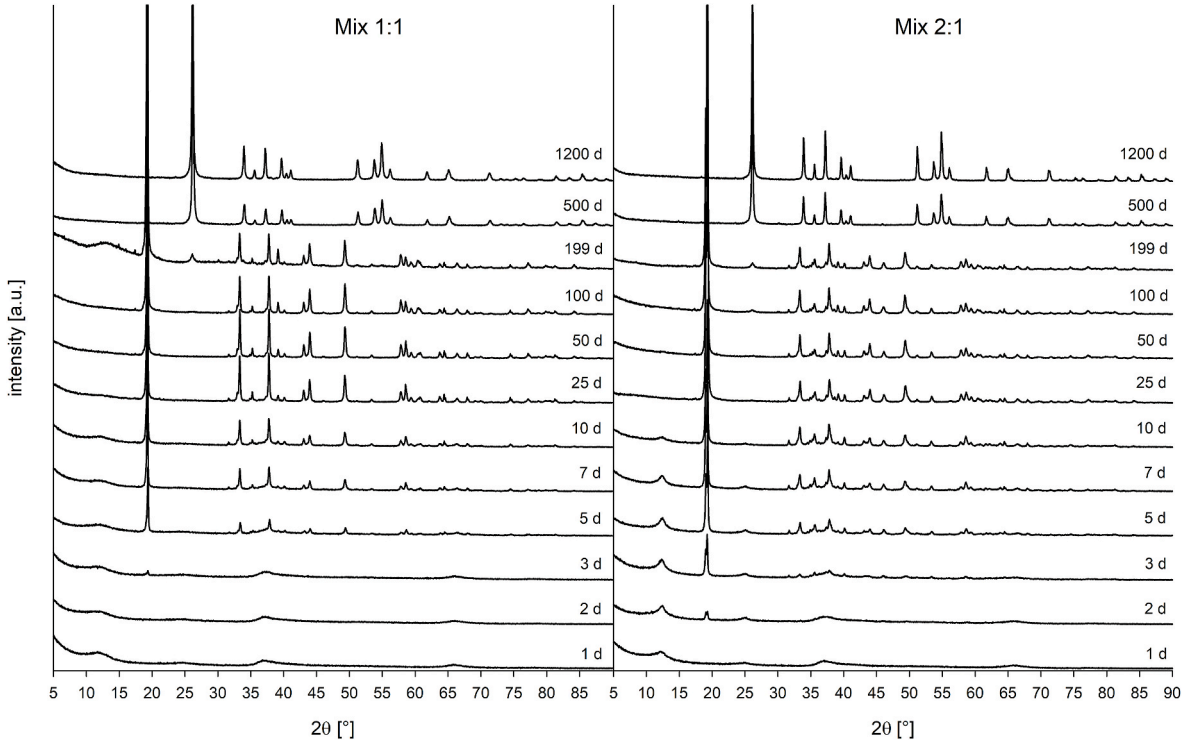

Fig. 1. XRD diffractograms from the precipitate of Mix 1:1 (left) and Mix 2:1 (right) for all time steps.

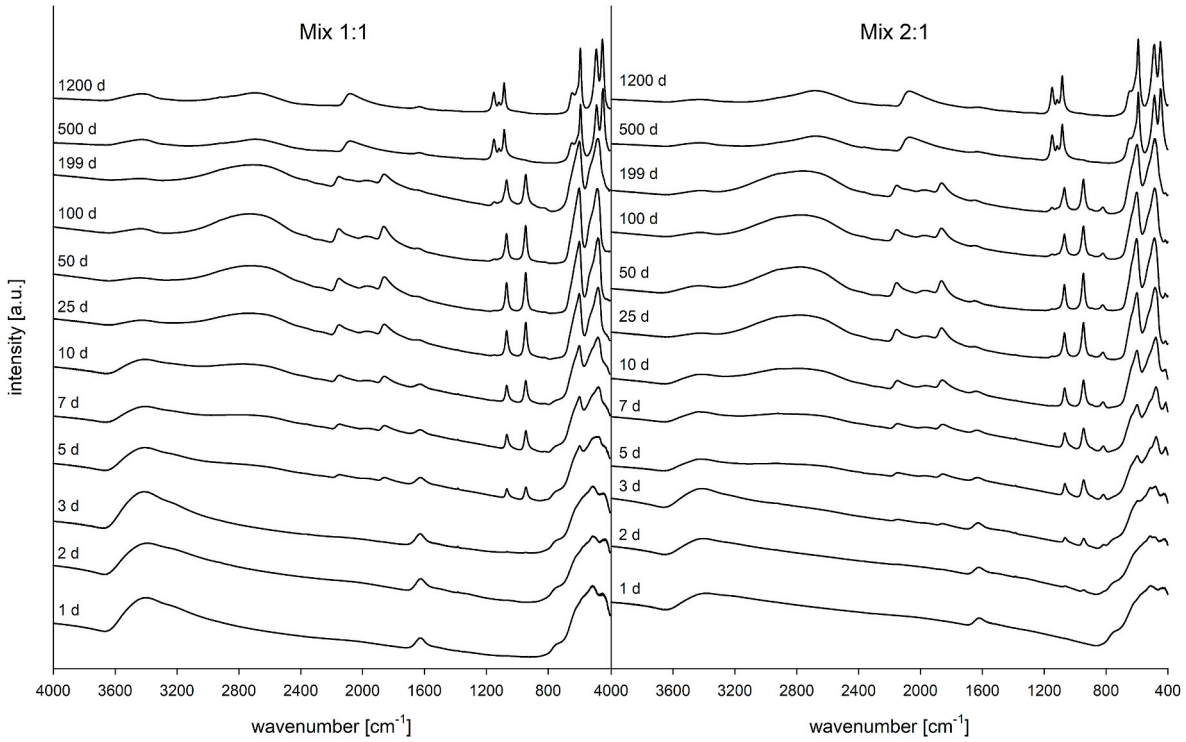

Fig. 2. FTIR spectra from the precipitate of Mix 1:1 (left) and Mix 2:1 (right) for all time steps.

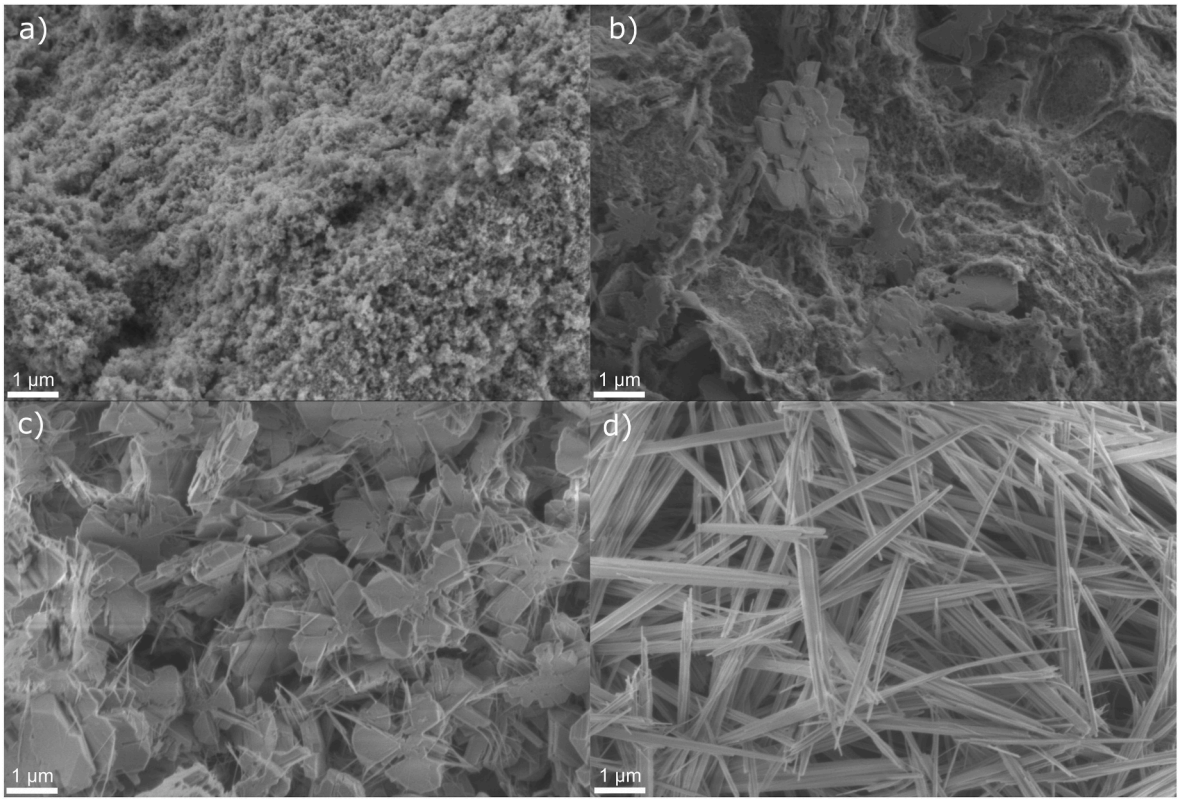

Fig. 3. Secondary electron images from the synthesized manganese oxide phases of Mix 1:1 after 1 d (a), 10 d (b), 199 d (c) and 500 d (d).

591, 486, and 447 cm^{-1}. After 500 d, no reflexes and absorption bands corresponding to feitknechtite or other manganese phases are visible in Mix 1:1 and Mix 2:1. At the same time, the features of manganite have increased in their intensity. The transformation into manganite is also evident in the SEM images, where the feitknechtite sheets show emergent manganite crystals as tiny rod-shaped needles after 199 d (Fig. 3c) that have fully evolved into large manganite needles after 500 d (Fig. 3d, cf. Tu et al. (1994)). There is no further change in spectra and

morphology until 1200 d.

3.2. Linear Combination Fit

The LCF was able to explain the features that appeared in both XRD diffractograms and FTIR spectra of pure mineral phases as well as their mixtures using the three components corresponding to birnessite, feitknechtite, and manganite (Fig. S5). As expected from the spectra in Mix 1:2, no signs of manganese phases other than birnessite are present in the LCF (Fig. 4). Low concentrations of any component, as seen in the LCF of Mix 1:2, can be caused by a component misassignment due to different background levels and, therefore, cannot be interpreted as traces of feitknechtite or manganite. However, three components are required in Mix 1:1 and Mix 2:1 to reconstruct the features in spectra and diffractograms, consistent with the previous interpretation of transformation in those mixtures. The FTIR component corresponding to birnessite disappears after 25 d in Mix 1:1 and after 10 d in Mix 2:1. Accordingly, the feitknechtite component is observed earlier and more pronounced when more lactate is present in Mix 2:1. A similar situation arises in the reconstruction of XRD data, where feitknechtite is visible after 2 d in Mix 2:1. Hence, high concentrations of LMWOA not only drive the transformation of birnessite phases after the precipitation of birnessite but also accelerate this transformation when available in excess as also seen in the first indications of feitknechtite sheets in SEM images after 1 d (Fig. S2). Due to the lack of samples between 200 d and 500 d, information about a potential increase in transformation rate from feitknechtite to manganite is not available in our data as pure manganite phases are present after 500 d in both XRD diffractograms and FTIR spectra (Figs. 1 and 2).

3.3. Role of low-molecular-weight organic acids

Considering the pH of around 9 in our experiments, we assumed that complete oxidation of organic acids yields dissolved HCO_3^- or CO_3^{2-}, and no CO_2 was released. Consequently, the carbon mass balance was closed in all treatments until 500 d, i.e., the sum of all measured dissolved (in) organic carbon species weighted by their carbon content remained constant and equal to the carbon initially provided with the lactate amendment (Fig. 5). Hence, oxalate, pyruvate, and acetate were the prominent LMWOA that participated in manganese reduction before they mineralized into inorganic carbon, and adsorption of (in)organic carbon to manganese oxides was negligible for the mass balance.

Lactate concentrations decreased in all three mixtures, but only Mix 1:2 showed total lactate consumption (Fig. 5) within the first day. Therefore, a molar ratio of lactate to MnO_4^- of 1:2 is insufficient to facilitate a mineral transformation beyond birnessite, and electrons from lactate oxidation are exhaustively used for permanganate reduction instead. Based on the stoichiometry of LMWOA oxidation (Fig. 6), we estimated that the amount of electrons released was about 10% higher than required for forming pure Mn^{IV}-birnessite, and some Mn^{III} is incorporated in the birnessite structure. In contrast to lactate and pyruvate, which are not detectable from the first day, considerable concentrations of oxalate and acetate were present over the duration of the experiment. However, they neither facilitated mineral transformations nor dissolution (Fig. 5). Hence, the oxidation of already highly oxidized LMWOA, such as oxalate and acetate, to reduce birnessite is not favored abiotically at alkaline pH values near 9 as used in our experiments. While Xyla et al. (1992) found a reductive dissolution of birnessite and feitknechtite with oxalate at pH values between 4 and 6, they also found a substantial decrease in the reaction rate at higher pH values. According to Xyla et al. (1992), the reductive dissolution of manganese oxides

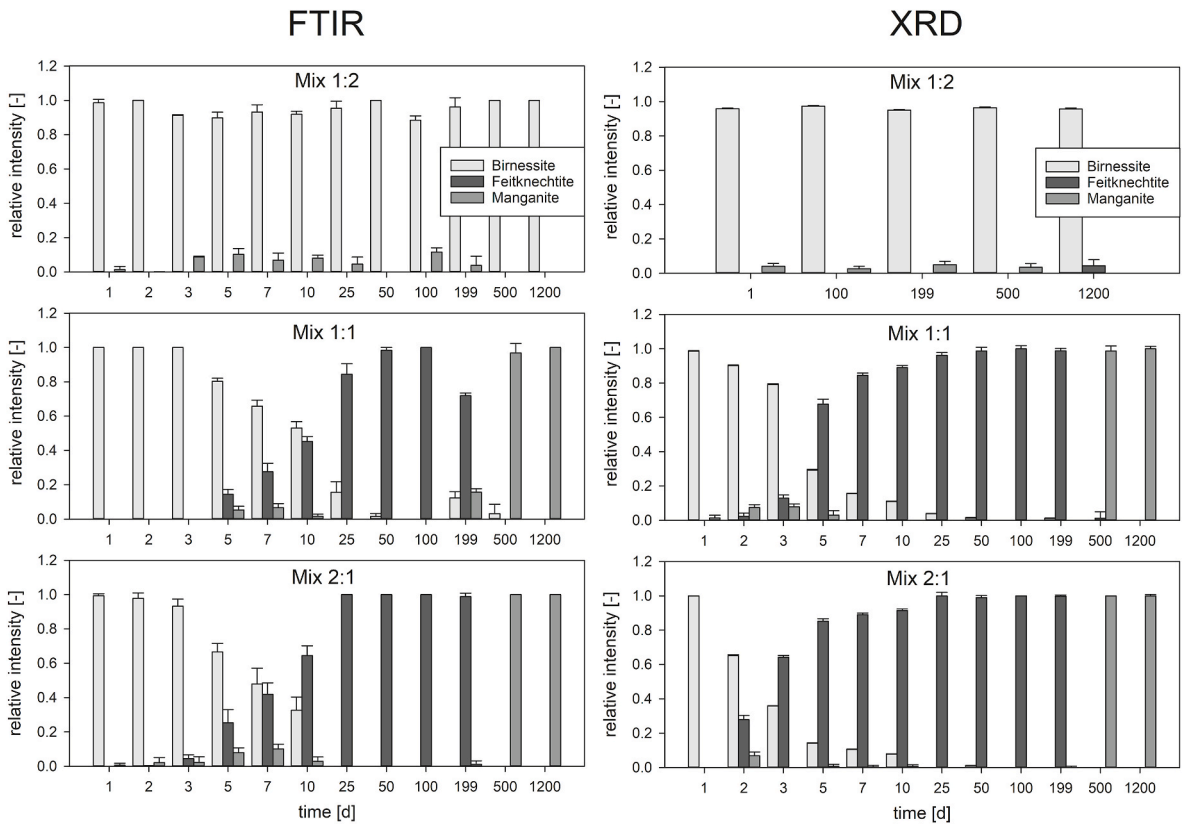

Fig. 4. Relative distribution of components from a Linear Combination Fit using spectra of pure birnessite, feitknechtite, and manganite for (left) FTIR data and (right) XRD data. Error bars indicate the standard deviation (n = 3) of experimental replicates for FTIR spectra and confidence intervals from the Linear Combination Fit for XRD diffractograms.

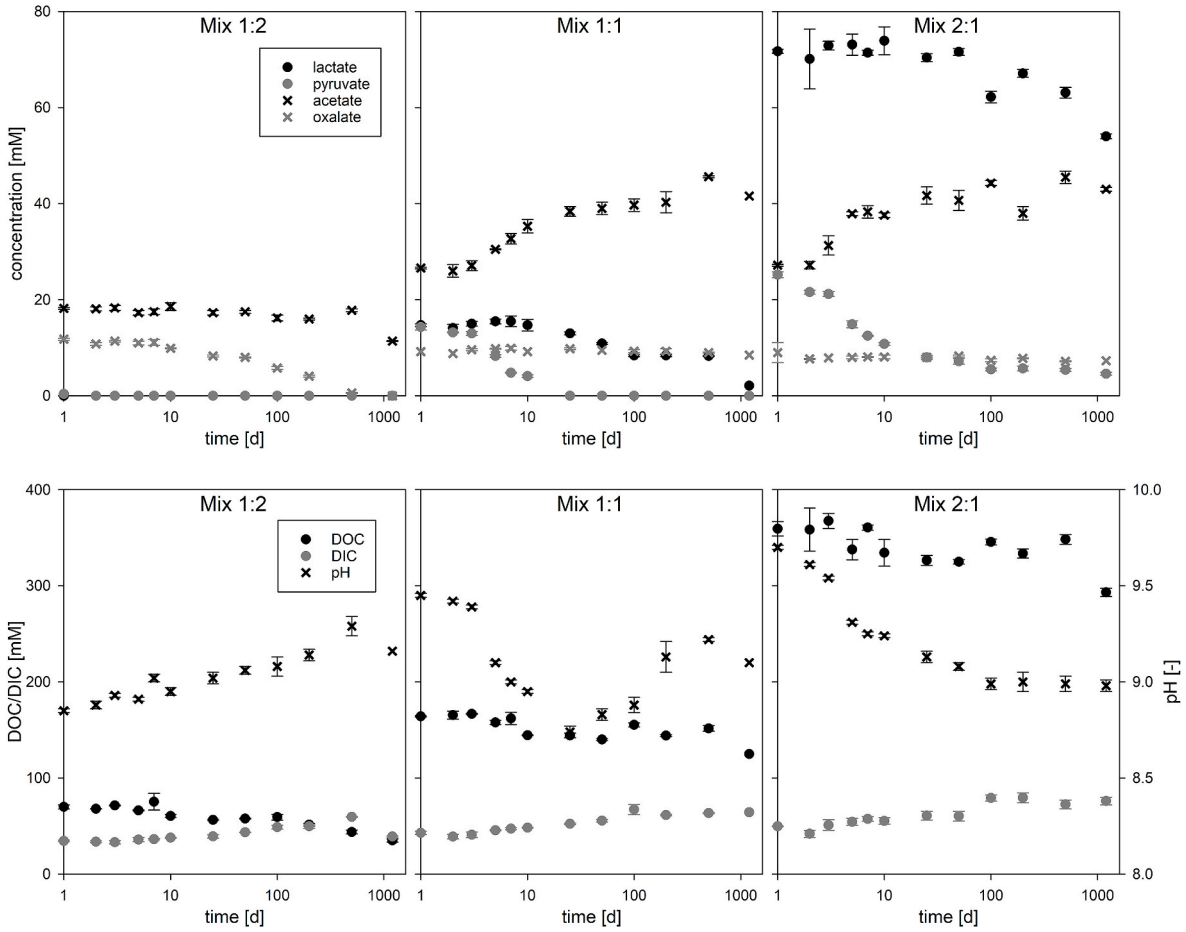

Fig. 5. Dissolved ions (top) and DOC/DIC/pH (bottom) for Mix 1:2 (left), Mix 1:1 (middle), and Mix 2:1 (right) in solution after the reaction of permanganate with lactate for 1–1200 d.

requires the formation of complexes between oxalate and manganese oxide surface moieties that do not form considerably when manganese oxide surfaces turn neutral or negative due to alkaline pH values. This finding is consistent with the results from Flynn and Catalano (2019), who only observed a change in birnessite crystallinity but no mineral transformation at neutral pH in response to oxalate.

When using higher initial lactate concentrations, the lactate concentration decreased by approximately 50 mM resulting in a concentration of 15 mM and 70 mM after one day in Mix 1:1 and Mix 2:1, respectively. Therefore, lactate is mainly oxidized within the first day for reducing Mn^{7+} in MnO_4^- to Mn^{4+}/Mn^{3+} with a high stoichiometric electron requirement compared to the reduction from Mn^{4+} to Mn^{3+}. The rapid initial decrease in lactate concentration within the first day mainly results from the reactivity of permanganate and the thermodynamic preference (Fig. 6) for birnessite (-322.6 kJ mol^{-1}). While the reduction of manganese continues after the first day, as seen in the formation of feitknechtite, the lactate concentration remains stable for ten days, and pyruvate is consumed instead. We explain this by the higher energy released from the oxidation of pyruvate to acetate (-171.75 kJ mol^{-1}) in comparison to lactate to pyruvate oxidation (-36.69 kJ mol^{-1}) or acetate to oxalate oxidation (-116.02 kJ mol^{-1}). Assuming that the reductive dissolution of manganese oxides is an initial step in manganese oxide transformation, the reductive dissolution rate due to different organic acids might be equally important. For instance, while Xyla et al. (1992) and Stone (1987) found that oxalate and pyruvate can reductively dissolve manganese oxides, Stone (1987) also showed that oxalate shows a more substantial decrease in the reaction rate with increasing pH than pyruvate. The lack of transformation observed in the presence of oxalate might be a consequence of its inability to reduce manganese oxides at alkaline pH at a measurable rate. In contrast, the reductive dissolution of manganese oxides by pyruvate might still be fast enough to permit the transformation observed in the timeframe of our experiments. During the pyruvate depletion, acetate is formed stoichiometrically, i.e., the sum of acetate and pyruvate stays constant. This period coincides with the formation of feitknechtite and shows that pyruvate is essential in manganese phase transitions. In Mix 1:1 and Mix 2:1, oxalate is present from the first day after initial lactate oxidation. It remains constant throughout the experiment, confirming that oxalate does not participate in phase transitions of manganese oxides at the experimental pH. The succession of LMWOA that are depleted and released is very similar in Mix 1:1 and Mix 2:1, and the increased lactate content in Mix 2:1 does not affect the general route of transformation.

The concentration of K^+ (originating from $KMnO_4$) was lower than provided initially but reached initial concentrations again in Mix 1:1 and 2:1 when birnessite was depleted (Fig. S6). This indicates that the transformation and recrystallization from birnessite to feitknechtite/manganite leads to a release of K^+ previously adsorbed to birnessite surfaces. The concentration of dissolved Mn^{2+} was below the detection limit of 0.001 mg L^{-1} during the entire experiment, and hence, no Mn^{2+} was released into the solution during the reaction. Therefore, the reduction of birnessite via LMWOA took place without dissolved Mn^{2+} having a considerable impact.

Yet, as the reductive dissolution of manganese phases is known to release Mn^{2+} at acidic pH values, a Mn^{2+}-induced reduction mechanism might also occur in our experiments. In that case, the lack of dissolved Mn^{2+} can be explained by its strong adsorption to manganese oxides at neutral to alkaline pH (Wang and Stone, 2006a). The similarity to the

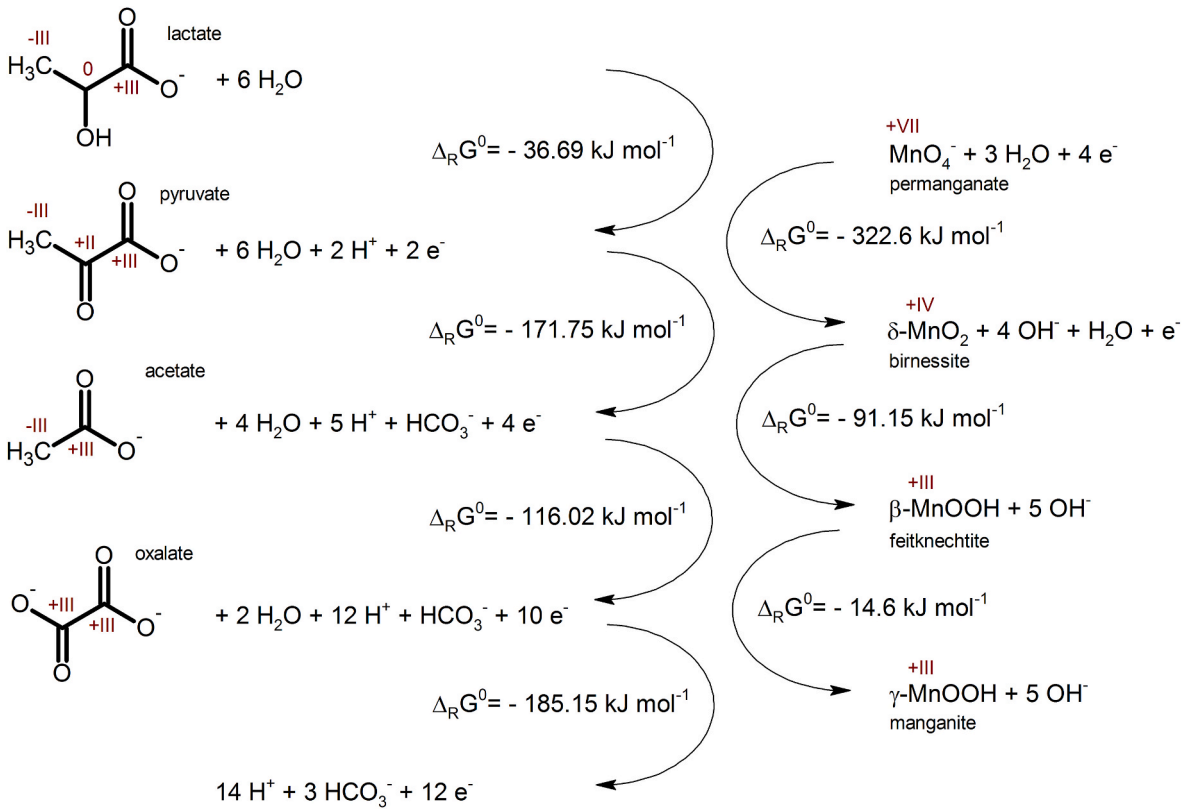

Fig. 6. Oxidation of LMWOA and reduction of manganese with changes in Gibbs Free Energy during reactions. Data on LMWOA and manganese phases were extracted from Goldberg and Alberty (2010) and Elzinga (2011).

transformation route found by Elzinga (2011) would then be a direct consequence of the comproportionation of adsorbed Mn^{2+} with Mn^{III}/Mn^{IV} oxides. We show that this can also happen by the in-situ release of Mn^{2+} after the reductive dissolution of manganese phases by LMWOA. Lefkowitz et al. (2013) also found hausmannite as a transformation product of birnessite by Mn^{2+} at alkaline pH, but they argued that this is likely a kinetic effect due to high Mn^{2+} concentrations that outcompete the formation of thermodynamically stable manganite. With the low Mn^{2+} concentrations and the timespan of 1200 d in our experiments, the transformation to manganite is consistent with those findings.

4. Conclusions

Our immediate results show that birnessite is reductively transformed to feitknechtite and manganite, with lactate and other LMWOA acting as reducing agents. This reaction is similar to the reductive transformation from birnessite to manganite as observed by Elzinga (2011), yet, it takes place without any Mn^{2+} being released into the solution and with LMWOA taking the role as electron donors. Since lactate and other LMWOA are often found in soil solutions (Strobel, 2001), their oxidation might constitute a significant route of pedogenic manganese mineral transformation. Usually, the concentrations of LMWOA in bulk soil solutions are relatively low (<1 mM), but upon rapid decomposition of plant residues (Drever and Vance, 1994) or near roots that typically exhibit LMWOA concentrations of 10–20 mM (Jones, 1998), high local LMWOA concentrations can be expected. While the turnover of LMWOA in soil is frequently attributed to microbial activity, their potential to reductively transform manganese (hydr)oxides could be another factor that limits the abundance of LMWOA in soil. Furthermore, LMWOA control the long-term stability of manganese phases in our experiments and, therefore, might also affect pedogenic manganese transformations considerably. If birnessite transforms into other manganese phases, the specific surface area decreases significantly (Händel et al., 2013a, 2013b), which limits the function of manganese minerals to act as a sink for both pollutants and nutrients. Like K in our experiments, adsorbed species are likely not retained during this transformation, posing a significant impact on the biogeochemical cycling of trace elements and the mobility of pollutants. While acidic conditions increase the reductive dissolution (Stone, 1987; Wang and Stone, 2006b), the alkaline pH values of our experiments favored the formation of feitknechtite and manganite (Elzinga, 2011; Lefkowitz et al., 2013). As manganese (hydr)oxides not only prevail in soils but also appear in limestone (Scopelliti and Russo, 2021) and other sedimentary rocks as crusts, the oxidation of LMWOA coupled with manganese reduction may accelerate host rock transformation and facilitate the alteration of surfaces, particularly in carbonate aquifers that feature high pH.

Author contribution statement

Kai Totsche: Conceptualization, Methodology, Resources, Validation, Funding acquisition, Writing- Reviewing and Editing. **Thomas Ritschel:** Methodology, Software, Visualization, Formal Analysis, Writing- Original draft preparation.

Declaration of competing interest

The authors declare that they have no known competing financial interests or personal relationships that could have appeared to influence the work reported in this paper.

Data availability

Data will be made available on request.

Acknowledgments

The authors thank Dr. Andreas Fritzsche and Dr. Tom Guhra for discussing FTIR and XRD data. We thank Dr. Matthias Händel and Stefan Brandt for their support in conducting the experiments and discussions. Financial support is acknowledged by the Deutsche Forschungsgemeinschaft within the framework of the research unit 2179 "MAD Soil - Microaggregates: Formation and turnover of the structural building blocks of soils" (Project no.: 193380941).

Appendix A. Supplementary data

Supplementary data to this article can be found online at https://doi.org/10.1016/j.chemosphere.2023.138414.

References

Anthony, J.W., Bideaux, R.A., Bladh, K.W., Nichols, M.C., 1997. Handbook of Mineralogy, vol. III. Mineralogical Society of America, Chant, USA.

Bargar, J.R., Fuller, C.C., Marcus, M.A., Brearley, A.J., Perez De la Rosa, M., Webb, S.M., Caldwell, W.A., 2009. Structural characterization of terrestrial microbial Mn oxides from Pinal Creek, AZ. Geochem. Cosmochim. Acta 73 (4), 889–910. https://doi.org/10.1016/j.gca.2008.10.036.

Borch, T., Kretzschmar, R., Kappler, A., Cappellen, P.V., Ginder-Vogel, M., Voegelin, A., Campbell, K., 2010. Biogeochemical redox processes and their impact on contaminant dynamics. Environ. Sci. Technol. 44 (1), 15–23. https://doi.org/10.1021/es9026248.

Bricker, O., 1965. Some stability relations in the system Mn-O_2-H_2O at 25° and one atmosphere total pressure. Am. Mineral. 50 (9), 1296–1354.

Buerger, M.J., 1936. The symmetry and crystal structure of manganite, Mn(OH)O. Z. für Kristallogr. - Cryst. Mater. 95 (1–6), 163–174. https://doi.org/10.1524/zkri.1936.95.1.163.

Burdige, D.J., Dhakar, S.P., Nealson, K.H., 1992. Effects of manganese oxide mineralogy on microbial and chemical manganese reduction. Geomicrobiol. J. 10 (1), 27–48. https://doi.org/10.1080/01490459209377902.

Drever, J.I., Vance, G.F., 1994. Role of soil organic acids in mineral weathering processes. In: Pittman, E.D., Lewan, M.D. (Eds.), Organic Acids in Geological Processes. Springer Berlin Heidelberg, pp. 138–161. https://doi.org/10.1007/978-3-642-78356-2_6.

Elzinga, E.J., 2011. Reductive transformation of birnessite by aqueous Mn(II). Environ. Sci. Technol. 45 (15), 6366–6372. https://doi.org/10.1021/es2013038.

Flynn, E.D., Catalano, J.G., 2019. Reductive transformations of layered manganese oxides by small organic acids and the fate of trace metals. Geochem. Cosmochim. Acta 250, 149–172. https://doi.org/10.1016/j.gca.2019.02.006.

Fritzsche, A., Pagels, B., Totsche, K.U., 2016. The composition of mobile matter in a floodplain topsoil: a comparative study with soil columns and field lysimeters. J. Plant Nutr. Soil Sci. 179 (1), 18–28. https://doi.org/10.1002/jpln.201500169.

Fritzsche, A., Ritschel, T., Schneider, L., Totsche, K.U., 2019. Identification and quantification of single constituents in groundwater with Fourier-transform infrared spectroscopy and Positive Matrix Factorization. Vib. Spectrosc. 100, 152–158. https://doi.org/10.1016/j.vibspec.2018.09.008.

Goldberg, R.N., Alberty, R.A., 2010. Standard transformed Gibbs energies of formation for biochemical reactants. In: Lide, D.R. (Ed.), CRC Handbook of Chemistry and Physics, 90th Edition. CRC Press/Taylor and Francis.

Händel, M., Rennert, T., Totsche, K.U., 2013a. A simple method to synthesize birnessite at ambient pressure and temperature. Geoderma 193–194, 117–121. https://doi.org/10.1016/j.geoderma.2012.09.002.

Händel, M., Rennert, T., Totsche, K.U., 2013b. Synthesis of cryptomelane- and birnessite-type manganese oxides at ambient pressure and temperature. J. Colloid Interface Sci. 405, 44–50. https://doi.org/10.1016/j.jcis.2013.05.041.

Hem, J.D., 1978. Redox processes at surfaces of manganese oxide and their effects on aqueous metal ions. Chem. Geol. 21 (3), 199–218. https://doi.org/10.1016/0009-2541(78)90045-1.

Hem, J.D., 1981. Rates of manganese oxidation in aqueous systems. Geochem. Cosmochim. Acta 45 (8), 1369–1374. https://doi.org/10.1016/0016-7037(81)90229-5.

Jones, D.L., 1998. Organic acids in the rhizosphere – a critical review. Plant Soil 205 (1), 25–44. https://doi.org/10.1023/A:1004356007312.

Jones, L.H.P., Milne, A.A., 1956. Birnessite, a new manganese oxide mineral from Aberdeenshire, Scotland. Mineral. Mag. J. Mineral Soc. 31 (235), 283–288. https://doi.org/10.1180/minmag.1956.031.235.01.

Jones, M.E., Nico, P.S., Ying, S., Regier, T., Thieme, J., Keiluweit, M., 2018. Manganese-driven carbon oxidation at oxic–anoxic Interfaces. Environ. Sci. Technol. 52 (21), 12349–12357. https://doi.org/10.1021/acs.est.8b03791.

Julien, C.M., Massot, M., Poinsignon, C., 2004. Lattice vibrations of manganese oxides: Part I. Periodic structures. Spectrochim. Acta Mol. Biomol. Spectrosc. 60 (3), 689–700. https://doi.org/10.1016/S1386-1425(03)00279-8.

Kohler, T., Armbruster, T., Libowitzky, E., 1997. Hydrogen bonding and Jahn–Teller distortion in groutite, α-MnOOH, and manganite, γ-MnOOH, and their relations to the manganese dioxides ramsdellite and pyrolusite. J. Solid State Chem. 133 (2), 486–500. https://doi.org/10.1006/jssc.1997.7516.

Lefkowitz, J.P., Rouff, A.A., Elzinga, E.J., 2013. Influence of pH on the reductive transformation of birnessite by aqueous Mn(II). Environ. Sci. Technol. 47 (18), 10364–10371. https://doi.org/10.1021/es402108d.

Lovley, D.R., 1991. Dissimilatory Fe(III) and Mn(IV) reduction. Microbiol. Rev. 55 (2), 259–287. https://doi.org/10.1128/mr.55.2.259-287.1991.

Luo, J., Huang, A., Park, S.H., Suib, S.L., O'Young, C.-L., 1998. Crystallization of sodium−birnessite and accompanied phase transformation. Chem. Mater. 10 (6), 1561–1568. https://doi.org/10.1021/cm970745c.

Madison, A.S., Tebo, B.M., Mucci, A., Sundby, B., Luther 3rd, G.W., 2013. Abundant porewater Mn(III) is a major component of the sedimentary redox system. Science 341 (6148), 875–878. https://doi.org/10.1126/science.1241396.

Mandernack, K.W., Post, J., Tebo, B.M., 1995. Manganese mineral formation by bacterial spores of the marine Bacillus, strain SG-1: evidence for the direct oxidation of Mn(II) to Mn(IV). Geochem. Cosmochim. Acta 59 (21), 4393–4408. https://doi.org/10.1016/0016-7037(95)00298-E.

Manning, B.A., Fendorf, S.E., Bostick, B., Suarez, D.L., 2002. Arsenic(III) oxidation and arsenic(V) adsorption reactions on synthetic birnessite. Environ. Sci. Technol. 36 (5), 976–981. https://doi.org/10.1021/es0110170.

Mansfeldt, T., 2004. Redox potential of bulk soil and soil solution concentration of nitrate, manganese, iron, and sulfate in two Gleysols. J. Plant Nutr. Soil Sci. 167 (1), 7–16. https://doi.org/10.1002/jpln.200321204.

McKenzie, R.M., 1971. The synthesis of birnessite, cryptomelane, and some other oxides and hydroxides of manganese. Mineral. Mag. 38 (296), 493–502. https://doi.org/10.1180/minmag.1971.038.296.12.

Nealson, K.H., Saffarini, D., 1994. Iron and manganese in anaerobic respiration: environmental significance, physiology, and regulation. Annu. Rev. Microbiol. 48 (1), 311–343. https://doi.org/10.1146/annurev.mi.48.100194.001523.

Novotnik, B., Zorz, J., Bryant, S., Strous, M., 2019. The effect of dissimilatory manganese reduction on lactate fermentation and microbial community assembly. Front. Microbiol. 10 https://doi.org/10.3389/fmicb.2019.01007.

Post, J.E., 1999. Manganese oxide minerals: crystal structures and economic and environmental significance. Proc. Natl. Acad. Sci. USA 96 (7), 3447–3454. https://doi.org/10.1073/pnas.96.7.3447.

Potter, R.M., Rossman, G.R., 1979. The tetravalent manganese oxides: identification, hydration, and structural relationships by infrared spectroscopy. Am. Mineral. 64 (11–12), 1199–1218.

Remucal, C.K., Ginder-Vogel, M., 2014. A critical review of the reactivity of manganese oxides with organic contaminants. Environ. Sci.: Process. Impacts 16 (6), 1247–1266. https://doi.org/10.1039/C3EM00703K.

Rennert, T., Pohlmeier, A., Mansfeldt, T., 2005. Oxidation of ferrocyanide by birnessite. Environ. Sci. Technol. 39 (3), 821–825. https://doi.org/10.1021/es040069x.

Ritschel, T., Totsche, K.U., 2017. Quantification of pH-dependent speciation of organic compounds with spectroscopy and chemometrics. Chemosphere 172, 175–184. https://doi.org/10.1016/j.chemosphere.2016.12.145.

Scopelliti, G., Russo, V., 2021. Petrographic and geochemical characterization of the Middle−Upper Jurassic Fe–Mn crusts and mineralizations from Monte Inici (north-western Sicily): genetic implications. Int. J. Earth Sci. 110 (2), 559–582. https://doi.org/10.1007/s00531-020-01971-0.

Stone, A.T., 1987. Microbial metabolites and the reductive dissolution of manganese oxides: oxalate and pyruvate. Geochem. Cosmochim. Acta 51 (4), 919–925. https://doi.org/10.1016/0016-7037(87)90105-0.

Strobel, B.W., 2001. Influence of vegetation on low-molecular-weight carboxylic acids in soil solution—a review. Geoderma 99 (3), 169–198. https://doi.org/10.1016/S0016-7061(00)00102-6.

Taylor, R.M., 1968. The associations of manganese and cobalt in soils - further observations. J. Soil Sci. 19 (1), 77–80. https://doi.org/10.1111/j.1365-2389.1968.tb01522.x.

Tebo, B.M., Bargar, J.R., Clement, B.G., Dick, G.J., Murray, K.J., Parker, D., Verity, R., Webb, S.M., 2004. Biogenic manganese oxides: properties and mechanisms of formation. Annu. Rev. Earth Planet Sci. 32 (1), 287–328. https://doi.org/10.1146/annurev.earth.32.101802.120213.

Tu, S., Racz, G.J., Goh, T.B., 1994. Transformations of synthetic birnessite as affected by pH and manganese concentration. Clay Clay Miner. 42 (3), 321–330. https://doi.org/10.1346/CCMN.1994.0420310.

Wang, Q., Yang, P., Zhu, M., 2018. Structural transformation of birnessite by fulvic acid under anoxic conditions. Environ. Sci. Technol. 52 (4), 1844–1853. https://doi.org/10.1021/acs.est.7b04379.

Wang, Y., Feng, X., Villalobos, M., Tan, W., Liu, F., 2012. Sorption behavior of heavy metals on birnessite: relationship with its Mn average oxidation state and implications for types of sorption sites. Chem. Geol. 292–293, 25–34. https://doi.org/10.1016/j.chemgeo.2011.11.001.

Wang, Y., Stone, A.T., 2006a. The citric acid–MnIII,IVO2(birnessite) reaction. Electron transfer, complex formation, and autocatalytic feedback. Geochem. Cosmochim. Acta 70 (17), 4463–4476. https://doi.org/10.1016/j.gca.2006.06.1551.

Wang, Y., Stone, A.T., 2006b. Reaction of MnIII,IV (hydr)oxides with oxalic acid, glyoxylic acid, phosphonoformic acid, and structurally-related organic compounds. Geochem. Cosmochim. Acta 70 (17), 4477–4490. https://doi.org/10.1016/j.gca.2006.06.1548.

Xyla, A.G., Sulzberger, B., Luther III, G.W., Hering, J.G., Van Cappellen, P., Stumm, W., 1992. Reductive dissolution of manganese(III, IV) (hydr)oxides by oxalate: the effect of pH and light. Langmuir 8 (1), 95–103. https://doi.org/10.1021/la00037a019.

Yang, P., Wen, K., Beyer, K.A., Xu, W., Wang, Q., Ma, D., Wu, J., Zhu, M., 2021. Inhibition of oxyanions on redox-driven transformation of layered manganese oxides. Environ. Sci. Technol. 55 (5), 3419–3429. https://doi.org/10.1021/acs.est.0c06310.